[redacted]

Copy 5
RM L54G22a

NACA

RESEARCH MEMORANDUM

LOW-SPEED MEASUREMENT OF STATIC STABILITY AND DAMPING DERIVATIVES OF A 60° DELTA-WING MODEL FOR ANGLES OF ATTACK OF 0° TO 90°

By Donald E. Hewes

Langley Aeronautical Laboratory
Langley Field, Va.

NATIONAL ADVISORY COMMITTEE FOR AERONAUTICS
WASHINGTON
September 14, 1954

[redacted]

[redacted]

NATIONAL ADVISORY COMMITTEE FOR AERONAUTICS

RESEARCH MEMORANDUM

LOW-SPEED MEASUREMENT OF STATIC STABILITY AND DAMPING DERIVATIVES OF A 60° DELTA-WING MODEL FOR ANGLES OF ATTACK OF 0° TO 90°

By Donald E. Hewes

SUMMARY

The static stability, control characteristics, and the damping in roll and yaw about the body axes of a 60° delta-wing model with two vertical-tail arrangements were measured for angles of attack of 0° to 90° to provide general information for studies of vertically rising jet-propelled airplanes. The damping derivatives were determined by the free-to-damp oscillation technique. The tests showed that a slightly unstable pitch-up tendency occurred at an angle of attack of about 35°. The effective dihedral of the model was positive except for angles of attack near 30°. A vertical tail mounted on top of the fuselage was effective as a stabilizing surface in sideslip for angles of attack up to only 35°; whereas a tail mounted on the bottom of the fuselage with the top tail on was effective throughout the angle-of-attack range. Effectiveness of the control surfaces decreased to very low values at the high angles of attack. The model maintained positive damping in roll and yaw about the body axes throughout the angle-of-attack range.

INTRODUCTION

The development of turbojet engines with very large thrust-to-weight ratios has made it possible to consider jet-propelled airplanes capable of being supported in hovering flight by the thrust of the engine. Very little information is available, however, on the aerodynamic characteristics of such airplanes for the hovering and transition phases of flight, that is, from the stall to an angle of attack of 90°. An investigation is being conducted by the National Advisory Committee For Aeronautics in order to provide information on which preliminary studies of the stability and handling qualities of airplanes of this type can be based. This investigation consists of static force tests and oscillation tests to measure the stability and control characteristics of existing models of straight-, sweptback-, and delta-wing airplanes which are generally representative of possible configurations for vertically rising airplanes.

[redacted]

In the present investigation, measurements were made of the static stability, control effectiveness, and damping derivatives of a delta-wing configuration for angles of attack of 0° to 90°. The configuration consisted of a fuselage with a 60° delta wing and either a single 60° delta vertical tail on the top of the fuselage or two 60° delta tails, one on the top and the other on the bottom of the fuselage. The tests were made in the Langley free-flight tunnel with specially constructed equipment which permitted the tests to be made over the angle-of-attack range from 0° to 90°.

SYMBOLS

All forces and moments are referred to the system of body axes which originate at the reference center-of-gravity location of the model at the 0.30 mean-aerodynamic-chord position. The system of axes and the directions of positive forces, moments, and angles are shown in figure 1.

a	logarithmic decrement, per second
b	span, ft
$\bar{c}$	mean aerodynamic chord, ft
k	torsional spring constant, ft-lb/radian
q	dynamic pressure, lb/ft^2
V	free-stream velocity, ft/sec
u,v,w	velocity components along the X, Y, and Z body axes, respectively, ft/sec
$p,\dot{\phi}$	rolling velocity, $\frac{d\phi}{dt}$, radians/sec
$r,\dot{\psi}$	yawing velocity, $\frac{d\psi}{dt}$, radians/sec
ω	circular frequency of oscillation, radians/sec
t	time, sec
α	angle of attack, $\tan^{-1}\frac{w}{u}$, deg
β	angle of sideslip, $\sin^{-1}\frac{v}{V}$, deg

ψ angle of yaw about Z body axis, deg or radians

ϕ angle of roll about X body axis, deg or radians

θ angle of pitch, deg (The relationship between θ and α is given by equation (1). When ϕ and ψ are zero, $\theta = \alpha$)

I_Z moment of inertia about Z body axis, slug-ft^2

I_X moment of inertia about X body axis, slug-ft^2

δ_a aileron deflection angle, deg

δ_e elevator deflection angle, deg

δ_r rudder deflection angle, deg

Z normal force, positive in direction of Z-axis, lb

X longitudinal force, positive in direction of X-axis, lb

Y lateral force, force directed along Y-axis, lb

M pitching moment, ft-lb

N yawing moment, ft-lb

L rolling moment, ft-lb

C_Z normal-force coefficient, Z/qS

C_X longitudinal-force coefficient, X/qS

C_Y lateral-force coefficient, Y/qS

C_m pitching-moment coefficient, $M/qS\bar{c}$

C_n yawing-moment coefficient, N/qSb

C_l rolling-moment coefficient, L/qSb

$N_\psi = \frac{\partial N}{\partial \psi}$ per radian

$N_r = \frac{\partial N}{\partial \frac{d\psi}{dt}}$ per deg or radians per sec

$C_{Z_\delta} = \frac{\partial C_Z}{\partial \delta}$ per deg

$C_{X_\delta} = \frac{\partial C_X}{\partial \delta}$ per deg

$C_{m_\delta} = \frac{\partial C_m}{\partial \delta}$ per deg

$C_{Y_\delta} = \frac{\partial C_Y}{\partial \delta}$ per deg

$C_{l_\delta} = \frac{\partial C_l}{\partial \delta}$ per deg

$C_{n_\delta} = \frac{\partial C_n}{\partial \delta}$ per deg

$C_{Y_\psi} = \frac{\partial C_Y}{\partial \psi}$ per deg

$C_{l_\psi} = \frac{\partial C_l}{\partial \psi}$ per deg

$C_{n_\psi} = \frac{\partial C_n}{\partial \psi}$ per deg

$C_{Y_\phi} = \frac{\partial C_Y}{\partial \phi}$ per deg

$C_{l_\phi} = \frac{\partial C_l}{\partial \phi}$ per deg

$C_{n_\phi} = \frac{\partial C_n}{\partial \phi}$ per deg

$$C_{Y_\beta} = \frac{\partial C_Y}{\partial \beta} \text{ per deg}$$

$$C_{n_\beta} = \frac{\partial C_n}{\partial \beta} \text{ per deg}$$

$$C_{l_\beta} = \frac{\partial C_l}{\partial \beta} \text{ per deg}$$

$$C_{n_{\dot{\beta}}} = \frac{\partial C_n}{\partial \frac{\dot{\beta} b}{2V}} \text{ per deg}$$

$$C_{l_{\dot{\beta}}} = \frac{\partial C_l}{\partial \frac{\dot{\beta} b}{2V}} \text{ per deg}$$

$$C_{l_p} = \frac{\partial C_l}{\partial \frac{pb}{2V}}$$

$$C_{n_r} = \frac{\partial C_n}{\partial \frac{rb}{2V}}$$

Subscripts:

f	friction of oscillating apparatus
0	initial condition at $t = 0$
r	right
l	left

SYSTEM OF AXES

All the data are presented with reference to the system of body axes about which the data were measured. This system of axes was chosen because it was felt that the motions of an airplane at very high pitch angles would be interpreted or sensed by the pilot relative to the body axes of the airplane. Also, the initial rolling motion of an airplane

during an aileron roll tends to be about the axis of least inertia, that is, the principal axis of inertia which generally is fairly closely alined with the X body axis.

The sequence by which the body axes are displaced from the reference axes, in this case, the tunnel axes, is important and was specified for this investigation as follows: with the two systems of axes initially alined, (1) pitch the model about Y-axis through the angle θ, (2) yaw about Z body axis through the angle ψ, and (3) roll about X body axis through the angle ϕ. The relations of θ, ψ, and ϕ to α and β for this sequence are as follows:

$$\left.\begin{aligned} \tan \alpha = \frac{w}{u} &= \tan \theta \frac{\cos \phi}{\cos \psi} + \tan \psi \sin \phi \\ \sin \beta = \frac{v}{V} &= \sin \theta \sin \phi - \cos \theta \sin \psi \cos \phi \end{aligned}\right\} \quad (1)$$

which reduce to the following approximations when it is assumed that ϕ and ψ are small and are varied separately:

$$\left.\begin{aligned} \alpha &= \theta \\ \beta &= \phi \sin \theta \\ \beta &= -\psi \cos \theta \end{aligned}\right\} \quad (2)$$

The sideslip derivatives, C_{Y_β}, C_{n_β}, and C_{l_β}, can be determined from the slopes, C_{Y_ϕ}, C_{n_ϕ}, C_{l_ϕ}, and so forth, of the wind-tunnel data by using the relations given in equations (2):

$$\left.\begin{aligned} C_{Y_\beta} &\approx \frac{C_{Y_\phi}}{\sin \theta} \approx \frac{-C_{Y_\psi}}{\cos \theta} \\ C_{n_\beta} &\approx \frac{C_{n_\phi}}{\sin \theta} \approx \frac{-C_{n_\psi}}{\cos \theta} \\ C_{l_\beta} &\approx \frac{C_{l_\phi}}{\sin \theta} \approx \frac{-C_{l_\psi}}{\cos \theta} \end{aligned}\right\} \quad (3)$$

The damping moments developed during a yawing oscillation are produced by the yawing velocity through the damping derivative C_{n_r} and by the rate of change of the sideslip angle through the damping derivative $C_{n_{\dot{\beta}}}$. For wind-tunnel tests at an angle of pitch of 0° where $\beta = -\psi$ and $\dot{\beta} = -\dot{\psi} = -r$, the total damping is expressed as $C_{n_r} - C_{n_{\dot{\beta}}}$. As the pitch angle is changed from zero, however, the relation between $\dot{\beta}$ and $\dot{\psi}$ is as determined from equation (2), $\dot{\beta} = -\dot{\psi} \cos \theta$. The expression for the total damping for any pitch angle therefore is

$$C_{n_r} - C_{n_{\dot{\beta}}} \cos \theta \tag{4}$$

In a similar manner, the total damping in roll is shown to be

$$C_{l_p} + C_{l_{\dot{\beta}}} \sin \theta \tag{5}$$

APPARATUS

The static force tests and oscillation tests were conducted in the Langley free-flight tunnel which is a low-speed tunnel with a 12-foot octagonal test section. The tunnel was designed primarily for flying dynamically scaled models but force testing and free-to-damp oscillation equipment have been installed so that the aerodynamic characteristics of models can be obtained.

A sketch of the model used in the investigation is given in figure 2 and a list of the pertinent dimensions is given in table I. The wing has a 60° delta plan form of aspect ratio 2.2 and two 60° delta vertical tails were used which could be mounted on the top and bottom of the fuselage. The area of each vertical tail was about 10 percent of the wing area.

Provisions were made in the model for attaching it to either of two internal three-component strain-gage balances at the reference center-of-gravity position. One of these balances was used to measure the forces X and Z and the moment M and the other was used to measure the lateral force Y and moments N and L. All forces and moments measured with these balances were relative to the body-axes system.

Static yaw force tests were made with the sting-type support system shown in figure 3. The model was mounted in the tunnel with the wing vertical and with the sting passing through the rear of the fuselage.

The pitch angle was changed by rotating the support about the vertical axis and the yaw angle was changed by rotating the sting in a vertical plane about an axis at the base of the sting. Remotely controlled electrical actuators were used for changing angles of pitch and yaw. Static roll force tests and damping tests were made with the support system shown in figure 4. For the static roll tests, the model was mounted the same as for the yaw force tests but, in this case, the sting was rotated so as to roll the model about its X body axis. In order to provide the oscillating system for the free-to-damp tests, a torsional spring was attached to the sting which was mounted in ball bearings. Sketches of the model mounted on the dynamic-test equipment for tests of the damping in yaw and roll are shown in figure 4. An inertia bar to which weights could be added was attached to the sting to provide a means of adjusting the number of cycles for the oscillation to damp. The angular position of the rotating sting was measured by means of a resistance slide-wire pickup connected to a recording galvanometer which traced the oscillations on recording paper.

TESTS

Static Tests

Force tests were made to determine the variations of C_Z, C_X, and C_m over the angle-of-pitch range from 0° to 90°. The variations of C_Y, C_n, and C_l with angle of yaw ($\pm 20^\circ$) and angle of roll ($\pm 20^\circ$) were determined at 10° increments of angle of pitch from 0° to 90° for the model with vertical tails off, with top tail on, and with both the top and bottom tails on.

Oscillation Tests

Free-to-damp oscillation tests were made to determine the total damping in roll and in yaw at 10° increments of angle of pitch from 0° to 90° for the model with vertical tails off, with the top tail on, and with both the top and bottom tails on. Weights were adjusted on the inertia bar so that at least four cycles of the oscillations were recorded for the tests in which the damping was a maximum. Four oscillation tests were usually recorded at each test point - a tare test with wind off to measure the residual friction damping of the system and three oscillation tests with wind on to measure the friction damping of the system plus the aerodynamic damping of the model. The oscillations were started by means of a light cable which was pulled and released by one of the tunnel operators. This cable remained attached to the sting when released but had a negligible effect on the damping. The model was displaced about 30° in bank or yaw before being released.

All static force tests and most of the oscillation tests were made at a dynamic pressure of about 3.9 pounds per square foot. A few oscillation check tests were made at a reduced pressure of 2.7 pounds per square foot. The tunnel velocities corresponding to these pressures were about 56 and 47 feet per second which gave Reynolds numbers of about 830,000 and 700,000, respectively. All the oscillation tests were made at a frequency of about 1 cycle per second.

DATA REDUCTION

All test data were reduced to standard nondimensional coefficient form. No corrections have been applied to the test data for strut tares, jet boundary, or tunnel blockage. The corrections, including the blockage correction for small pitch angles of the model, were considered to be negligible. Unpublished data have indicated that the corrections for tunnel blockage with the model at the high pitch angles may be large (of the order of 20 to 30 percent); however, it is believed that the trends of the data would not be altered appreciably if these corrections could be determined accurately and were applied to the data.

The damping derivatives were calculated from the test data by using the equations which were derived from the equation of motion for a damped single-degree-of-freedom system. For the case of the yawing oscillation, the equation of motion may be written as

$$\left[D^2 \frac{-(N_r - N_{\dot{\beta}} \cos\theta + N_{r_f})}{I_Z} D - \frac{N_\psi + K}{I_Z} \right] \psi = 0 \qquad (6)$$

where $D = \frac{d}{dt}$. The yawing motion of this system can be expressed by an equation of the form

$$\psi = e^{-at}(A \sin \omega t + B \cos \omega t) \qquad (7)$$

which represents a damped harmonic oscillation and where a and ω are the real and imaginary parts of the roots of equation (6). The envelope of this oscillation may be written

$$\psi_t = \psi_o e^{-at} \qquad (8)$$

[redacted]

where ψ_t is the amplitude at some time t following the initial amplitude ψ_o at $t = 0$. The value of a may be determined from

$$a = \frac{\log \psi_o - \log \psi_t}{t} \tag{9}$$

The expression for the damping terms is derived by substituting equation (8) into equation (6) and is

$$N_r - N_{\dot{\beta}} \cos \theta + N_{r_f} = -2I_Z a \tag{10}$$

The damping term due to friction of the test apparatus alone is

$$N_{r_f} = -2I_Z a_f \tag{11}$$

The aerodynamic-damping term is therefore

$$N_r - N_{\dot{\beta}} \cos \theta = -2I_Z(a - a_f) \tag{12}$$

or, expressed in nondimensional form,

$$C_{n_r} - C_{n_{\dot{\beta}}} \cos \theta = \frac{-4I_Z V(a - a_f)}{qSb^2} \tag{13}$$

The value of I_Z is determined from the following expression derived from equation (6) for the wind-off case when N_r and $N_{\dot{\beta}} \cos \theta$ terms are zero and the N_{r_f} term is negligible:

$$I_Z = \frac{-kP_n^2}{4\pi^2} \tag{14}$$

where P_n is the period of yawing oscillation.

The expression for the aerodynamic-damping term for the rolling oscillation is found in a similar manner to be

$$C_{l_p} + C_{l_{\dot{\beta}}} \sin \theta = \frac{-4I_X V(a - a_f)}{qSb^2} \tag{15}$$

and the value of I_X is found from

$$I_X = \frac{-kP_\ell^2}{4\pi^2} \tag{16}$$

where P_ℓ is the period of rolling oscillation.

The envelope of the oscillation was faired for each record obtained in the oscillation tests and plotted on semilogarithmic paper. Because of the turbulence of the airstream, and because of the nonviscous type of damping produced by the friction of the oscillation apparatus, the logarithmic envelope curve was nonlinear for the amplitudes of the oscillation below approximately $\pm 2^\circ$ or $\pm 3^\circ$. The value of a was therefore determined from the slope of the logarithmic envelope curve for the larger amplitudes. The moment of inertia of the system was calculated from the period of the oscillation obtained from the wind-off tests. An average value for the damping derivatives for each test point was determined from the test data. The spread in the test data was of the order of ±10 percent over the angle-of-pitch range except in the region of an angle of pitch of 30° where the spread was of the order of 20 percent.

RESULTS AND DISCUSSION

Longitudinal Characteristics

The variations with θ of the normal- and longitudinal-force and pitching-moment coefficients are shown in figure 5. The model was longitudinally unstable for pitch angles between about 35° and 50°. Figure 5 shows that the model could not be trimmed at pitch angles above 50° with the elevator deflection of -30°. The data presented in figure 6, which were obtained from figure 5, show that the elevator effectiveness at 90° was about one-half that at 0°.

Lateral Characteristics

The variations with ψ of the lateral force and moment coefficients are shown in figure 7 for the three configurations tested. The variations with ϕ of the lateral force and moments are shown in figure 8 for the configuration with the top tail on. The variations with pitch angle of the rolling and yawing moments at $\phi = 0$ and $\psi = 0$ which were obtained by cross-plotting data presented in figure 7 are shown in figure 9. Figure 9 shows that large out-of-trim moments were produced as the pitch angle was changed. This effect may be attributed partly to vortices generated by the nose of the fuselage. Reference 1 showed that

large out-of-trim yawing moments can be produced by a sharp nose body of revolution by the asymmetrical shedding of such vortices.

Static stability derivatives.- The variations with θ of the static roll and yaw stability derivatives are shown in figure 10. The values for the derivatives were determined from the data presented in figures 7 and 8 for amplitudes of ϕ and ψ of $\pm 5^{\circ}$. The sideslip derivatives are presented in figure 11 and were determined for amplitudes of β of $\pm 5^{\circ}$. The values for the sideslip derivatives were calculated from data presented in figure 7 and 8 by transforming the angles of ϕ and ψ into β by use of the relations given in equations (2). The values of the derivatives were calculated from the yaw data for pitch angles up to 60° and from the roll data for angles between 30° and 90°.

The curves of figure 11 show that the effective dihedral was positive $-C_{l_\beta}$ except for angles of pitch near 30° for all the configurations tested. The tail-off configuration was directionally unstable $-C_{n_\beta}$ throughout the pitch-angle range. The top tail was effective as a stabilizing surface up to an angle of pitch of about 35°, whereas the bottom tail with the top tail on was effective throughout the angle-of-pitch range tested. However, the model was directionally unstable throughout most of the range of pitch angles with either one or both tails on.

Lateral control.- The variations with θ of the increments in the lateral force and moment coefficients produced by deflecting the ailerons from 0° to -15° on the right and 15° on the left and deflecting the rudders from 0° to -25° are presented in figure 12. The ailerons maintained positive rolling power throughout the angle-of-pitch range, but the effectiveness decreased appreciably for the large angles of pitch. The ailerons produced favorable yawing moments for angles of pitch below about 50° and adverse moments above this angle. The rudder of the top vertical tail was ineffective for pitch angles above 45°; whereas the rudder of the bottom tail maintained some effectiveness throughout the angle-of-pitch range.

Damping derivatives.- Curves showing the variations with angle of pitch of the damping derivatives, $C_{l_p} + C_{l_{\dot{\beta}}} \sin\theta$ and $C_{n_r} - C_{n_{\dot{\beta}}} \cos\theta$, measured relative to the body axis are presented in figure 13.

The damping in roll of the model with tails off increased as the angle of pitch increased up to 30° and then decreased. The large change in the damping in the region of 30° coincides with the change in effective dihedral shown in figure 11. It is believed that these two factors are related inasmuch as a lag in the buildup and decay of the rolling moment produced by sideslipping during the rolling oscillation would cause the moment to lag the sideslip angle. In the case where C_{l_β} is

positive, as is the case in the region of 30° pitch angle, the rolling moment would be lagging and opposing the motion and, therefore, producing damping. This damping would be the contribution of $C_{l_{\dot{\beta}}} \sin \theta$ to the total damping. The top vertical tail reduced the damping of the tail-off configuration at angles of pitch up to about 30°. The bottom tail with the top tail on had very little effect throughout the angle-of-pitch range.

The damping in yaw of the tail-off configuration increased with angle of pitch up to pitch angles of 30° and then decreased. The change in the damping in the region of 30° is attributed partly to the contribution of $C_{n_{\dot{\beta}}} \cos \theta$ to the total damping by the same reasoning which was used to explain the change in damping in roll. The top vertical tail increased the damping for angles of pitch up to only about 45° but the bottom vertical tail with the top tail on increased the damping throughout the angle-of-pitch range.

SUMMARY OF RESULTS

The following results were obtained from the investigation of the static stability, control characteristics, and damping derivatives about the body axes of a 60° delta-wing model for the angle-of-pitch range of 0° to 90°:

1. The model was longitudinally unstable for pitch angles between about 35° and 50°.

2. The effective dihedral was positive except for angles of pitch near 30°.

3. The top vertical tail was effective as a stabilizing surface in sideslip for angles of pitch up to only about 35° whereas the bottom tail with the top tail on was effective throughout the angle-of-pitch range. The model, however, was directionally unstable throughout most of the range with either one or both tails on.

4. The elevators, ailerons, and the rudder of the bottom vertical tail were effective throughout the angle-of-pitch range although their effectiveness decreased at the larger pitch angles. The rudder of the top vertical tail was ineffective for angles of pitch above 45°.

5. The model maintained positive damping in roll and yaw about the body axes throughout the pitch-angle range for all three configurations tested.

Langley Aeronautical Laboratory,
National Advisory Committee for Aeronautics,
Langley Field, Va. July 8, 1954.

REFERENCE

1. Letko, William: A Low-Speed Experimental Study of the Directional Characteristics of a Sharp-Nosed Fuselage Through a Large Angle-of-Attack Range at Zero Angle of Sideslip. NACA TN 2911, 1953.

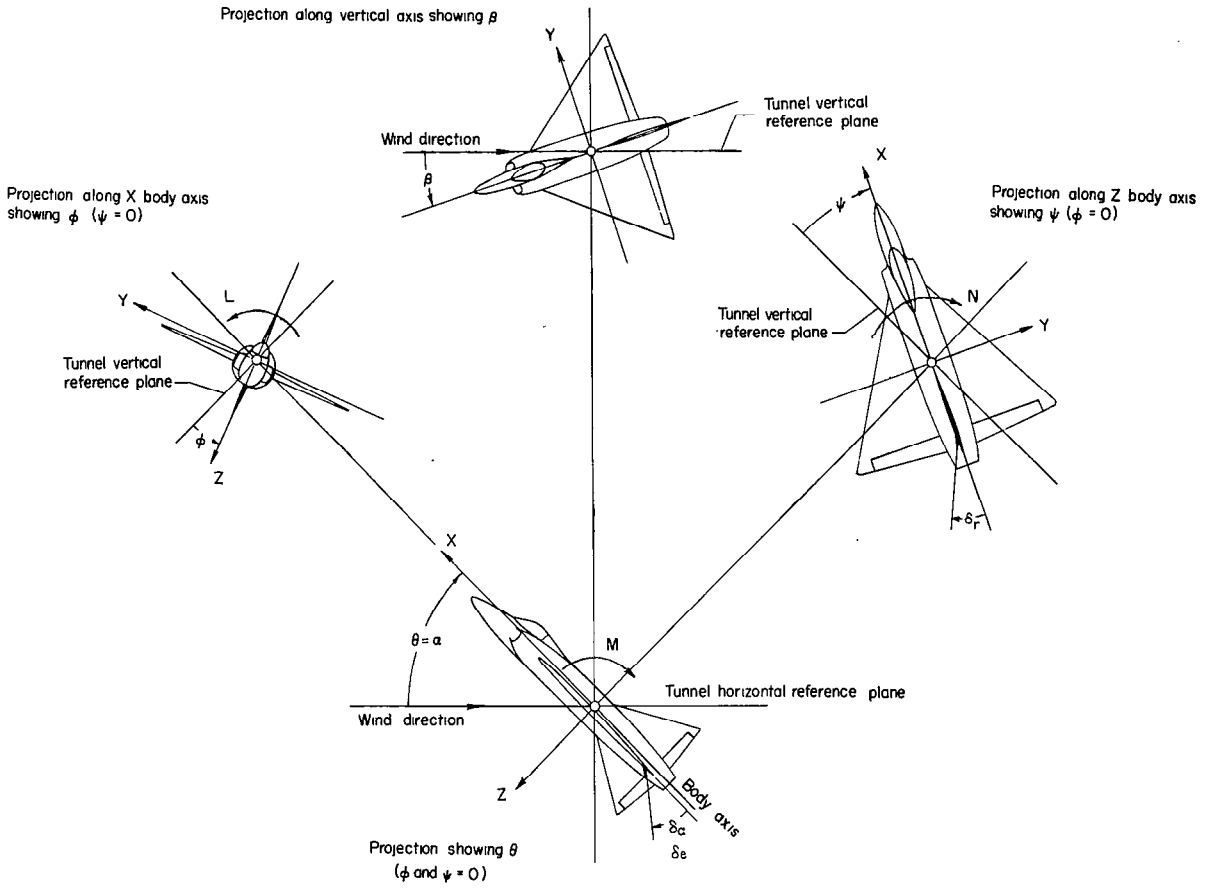

Figure 1.- The body system of axes. Arrows indicate positive directions of moments, forces, and angles. This system of axes is defined as an orthogonal system having the origin at the center of gravity and in which the X-axis is in the plane of symmetry and alined with the longitudinal axis of the fuselage, the Z-axis is in the plane of symmetry and perpendicular to the X-axis, and the Y-axis is perpendicular to the plane of symmetry.

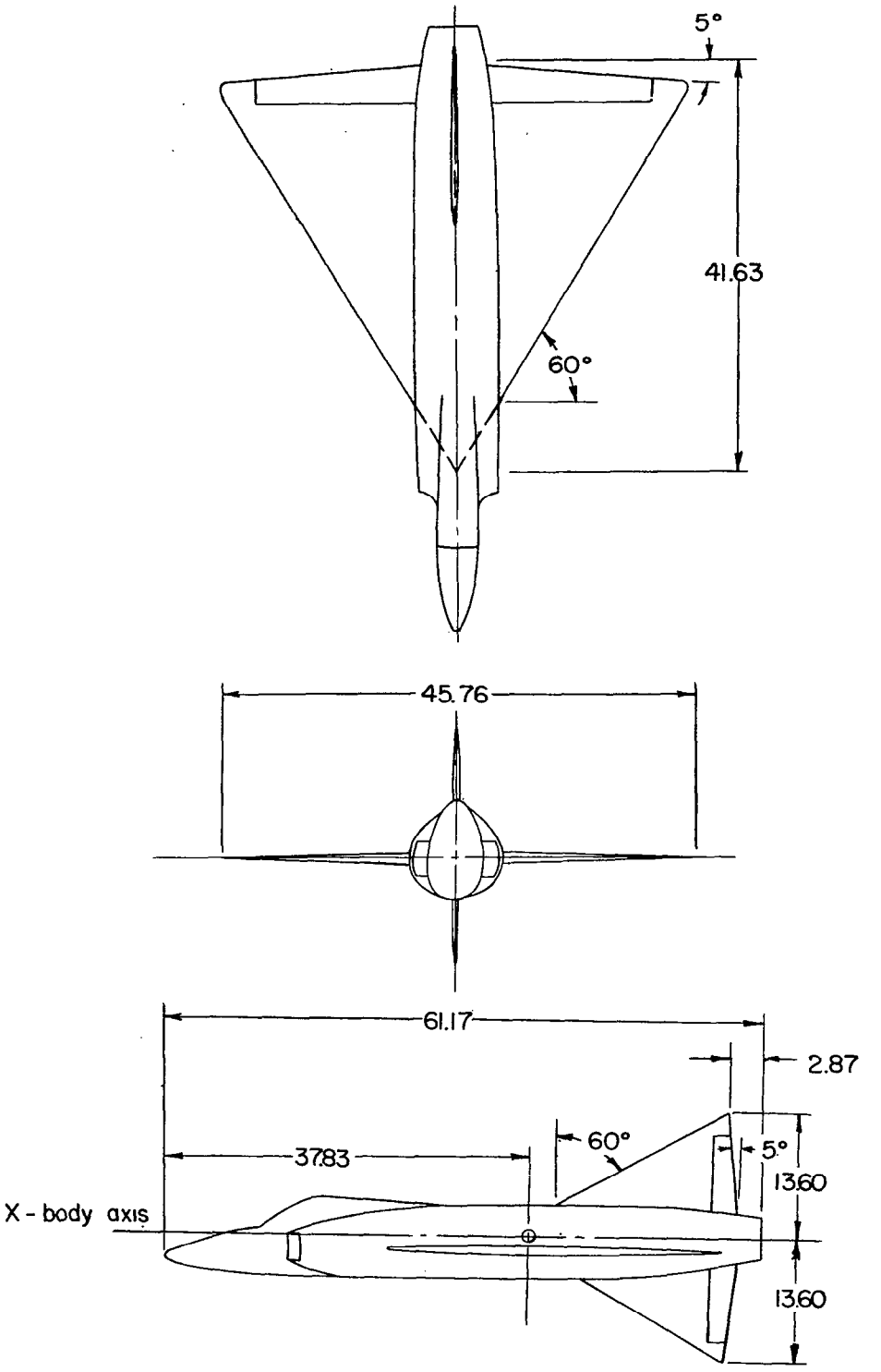

Figure 2.- Sketch of the delta-wing model used in the investigation. All dimensions are in inches.

L-84543

Figure 3.- Photograph of static-force-test equipment in the Langley free-flight tunnel with the model pitched and yawed.

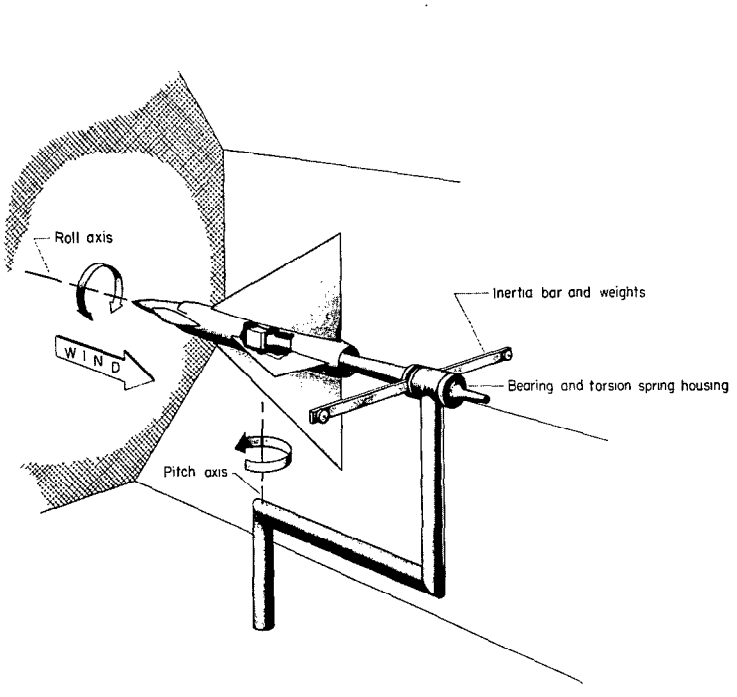

(a) Arrangement for damping-in-roll tests.

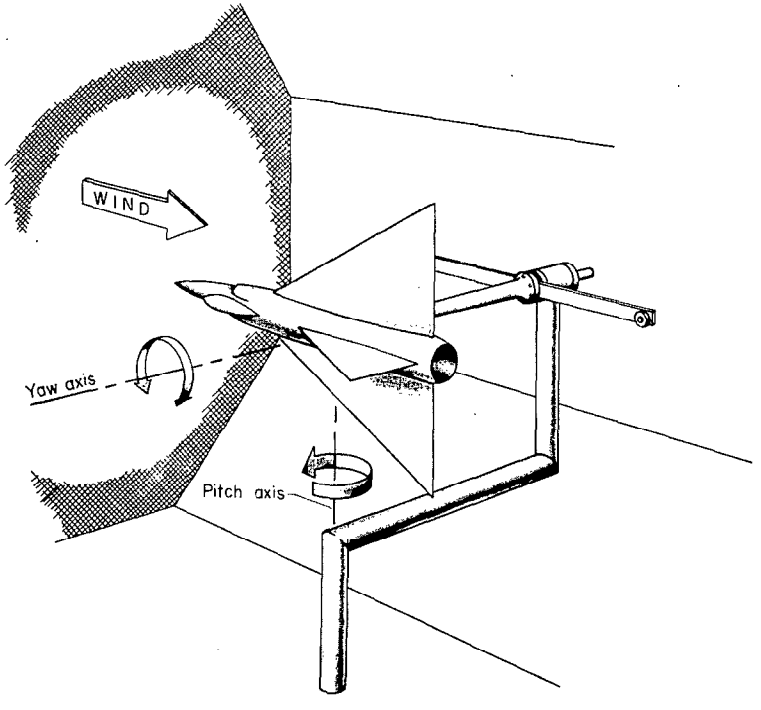

(b) Arrangement for damping-in-yaw tests.

L-85593

Figure 4.- Schematic sketch of model mounted on dynamic-test equipment.

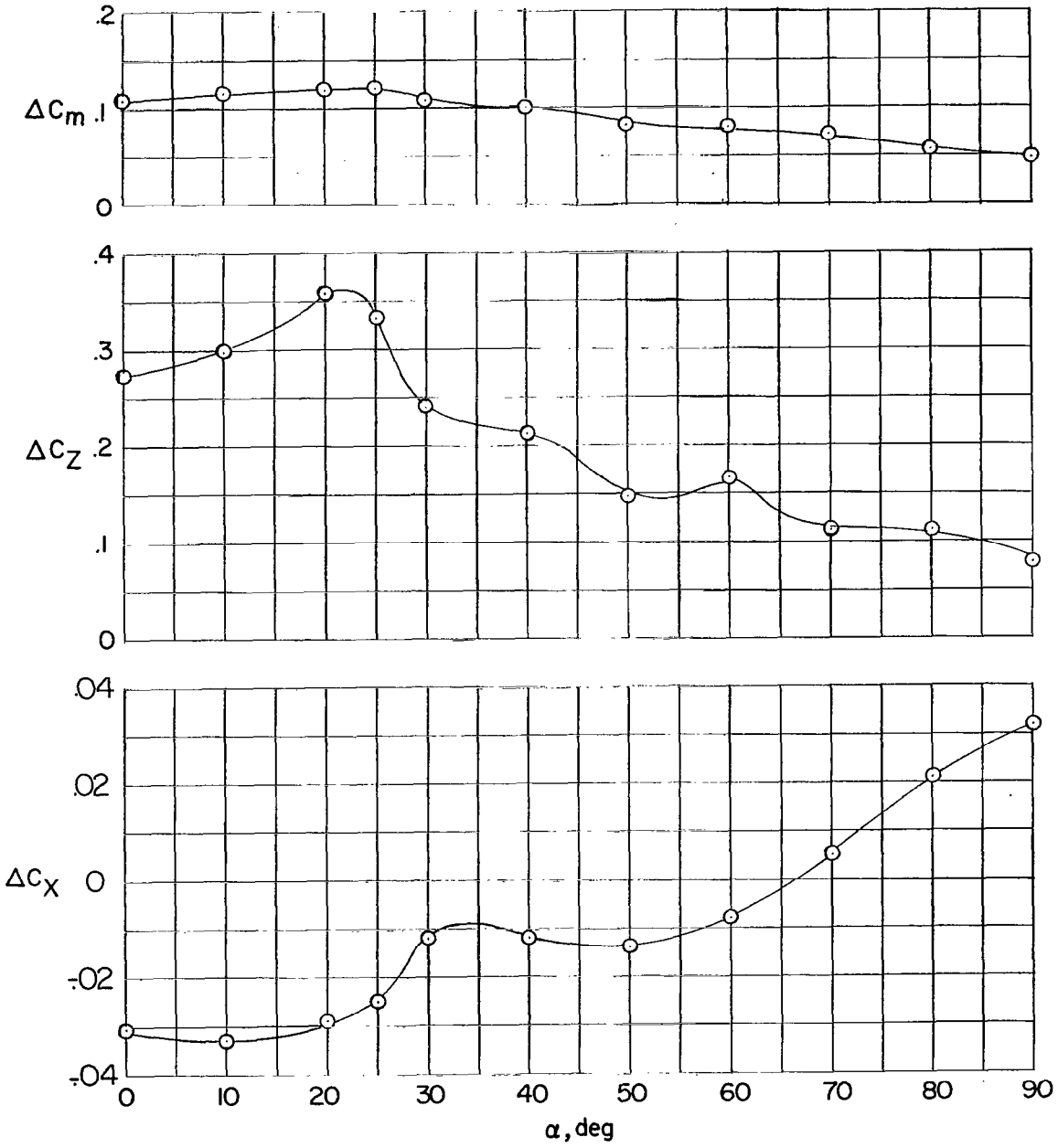

Figure 6.- Increments in the normal and longitudinal force and moment coefficients produced by deflecting elevators from 0° to -30°.

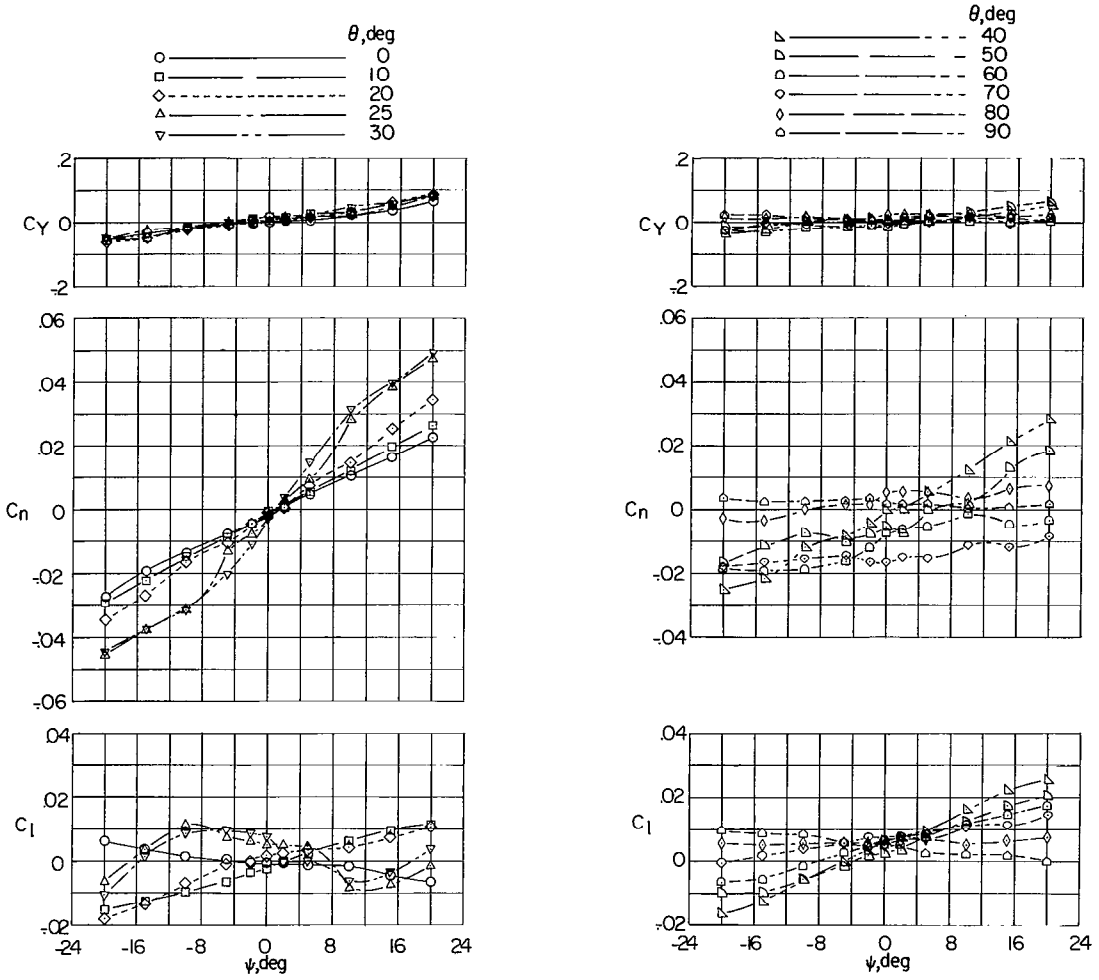

(a) Tails off.

Figure 7.- Static-force-test data showing the variation of lateral force, and yawing- and rolling-moment coefficients with angle of yaw.

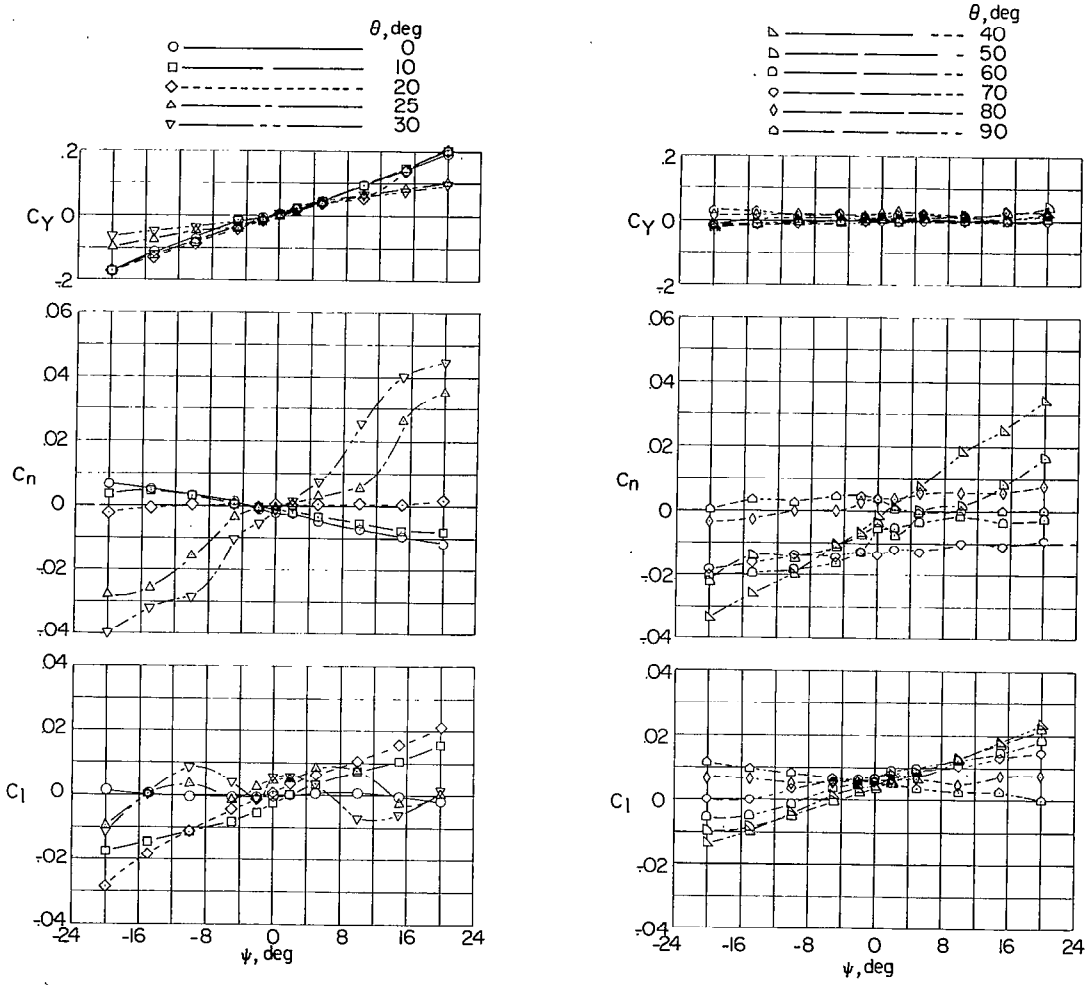

(b) Top vertical tail on.

Figure 7.- Continued.

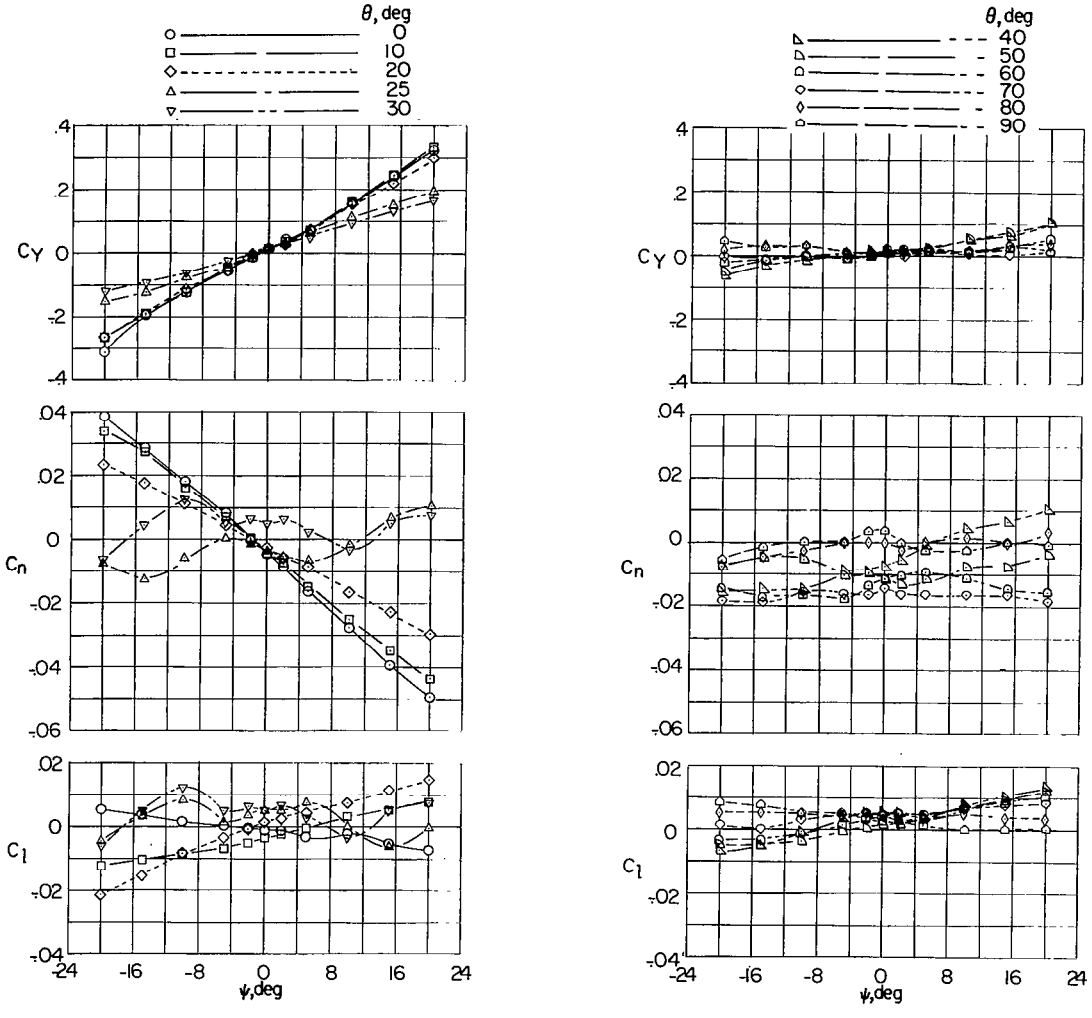

(c) Top and bottom vertical tails on.

Figure 7.- Concluded.

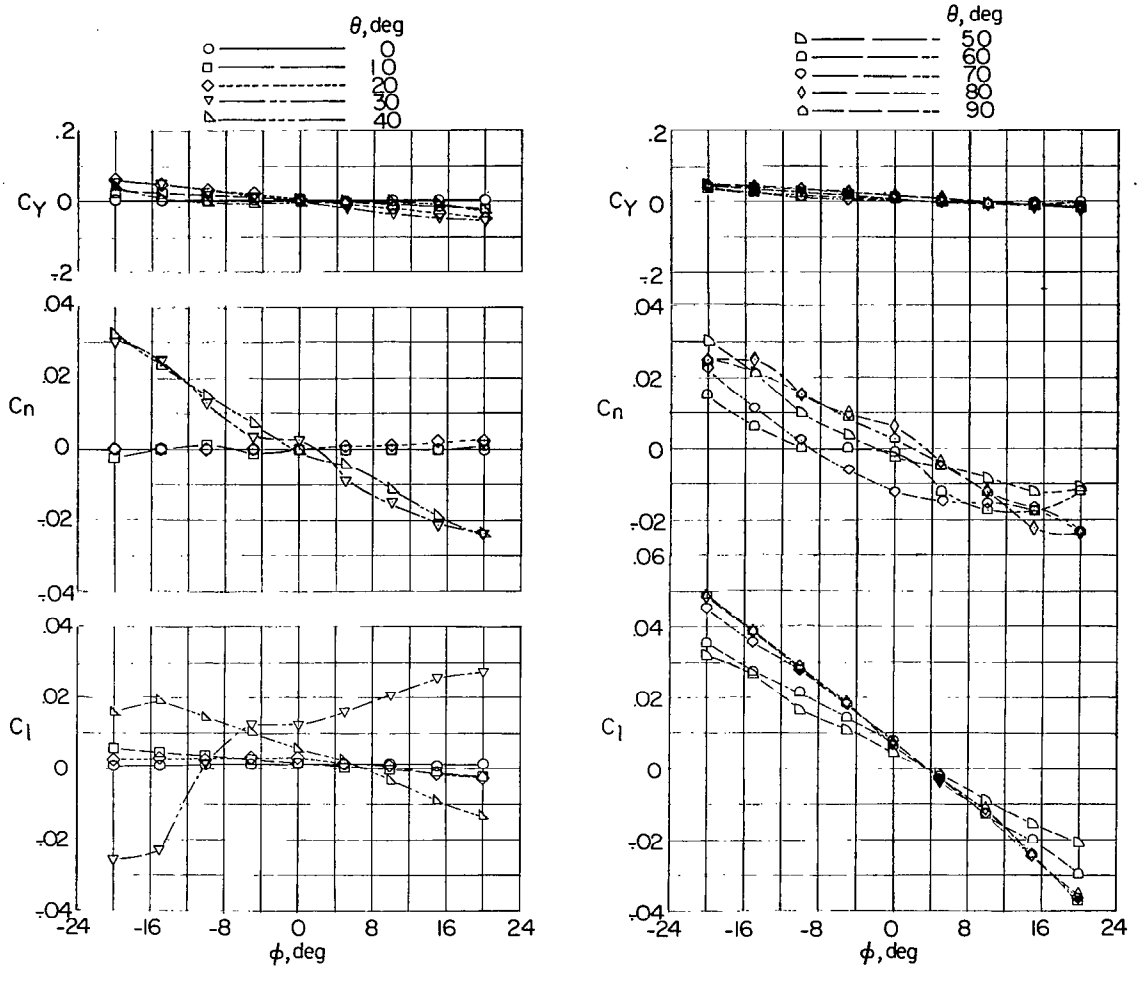

Figure 8.- Static-force-test data showing the variation of the lateral-force, yawing- and rolling-moment coefficients with angle of roll with top tail on.

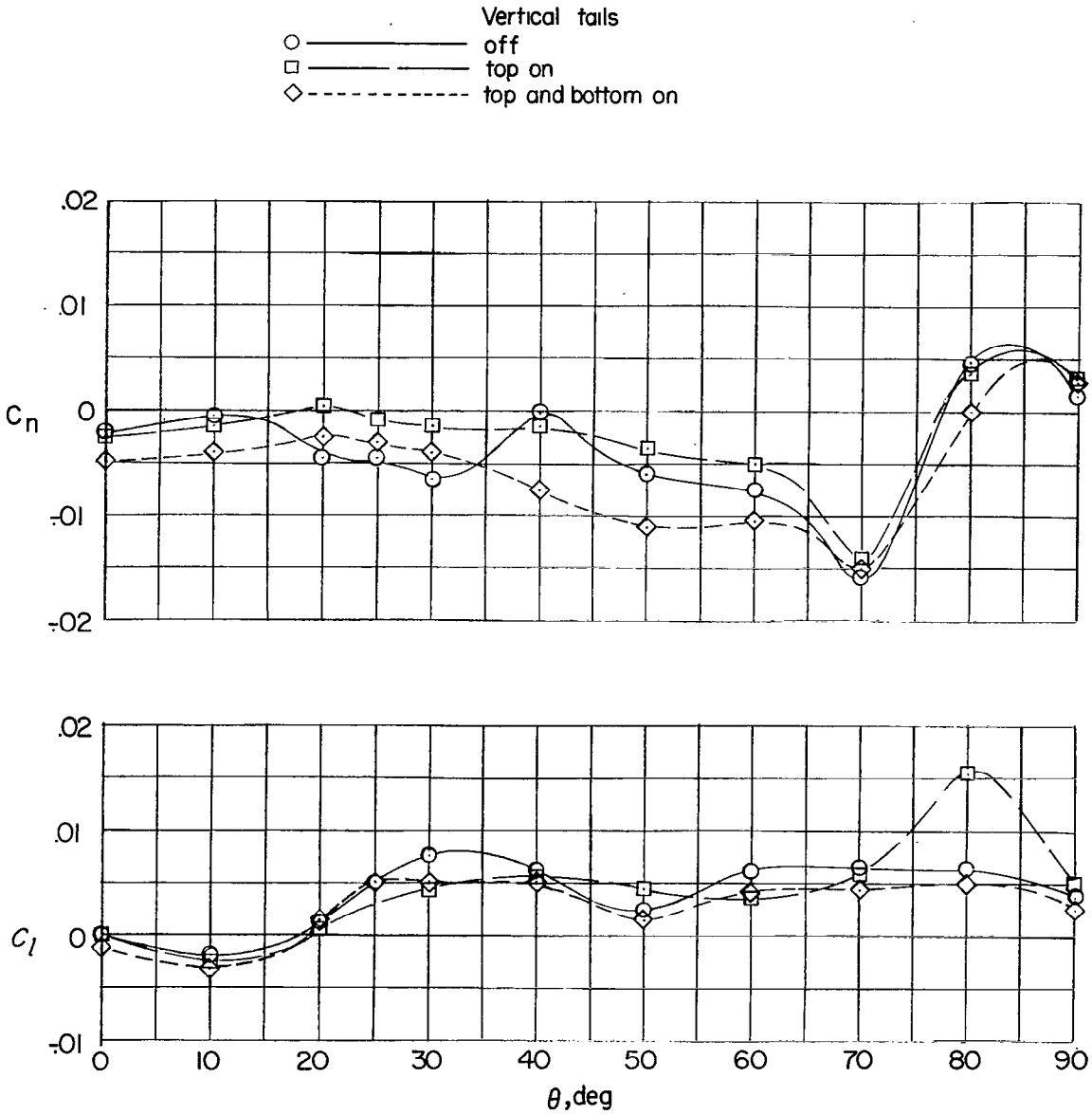

Figure 9.- Variation of yawing- and rolling-moment coefficients with angle of pitch for $\psi = 0^\circ$ and $\phi = 0^\circ$.

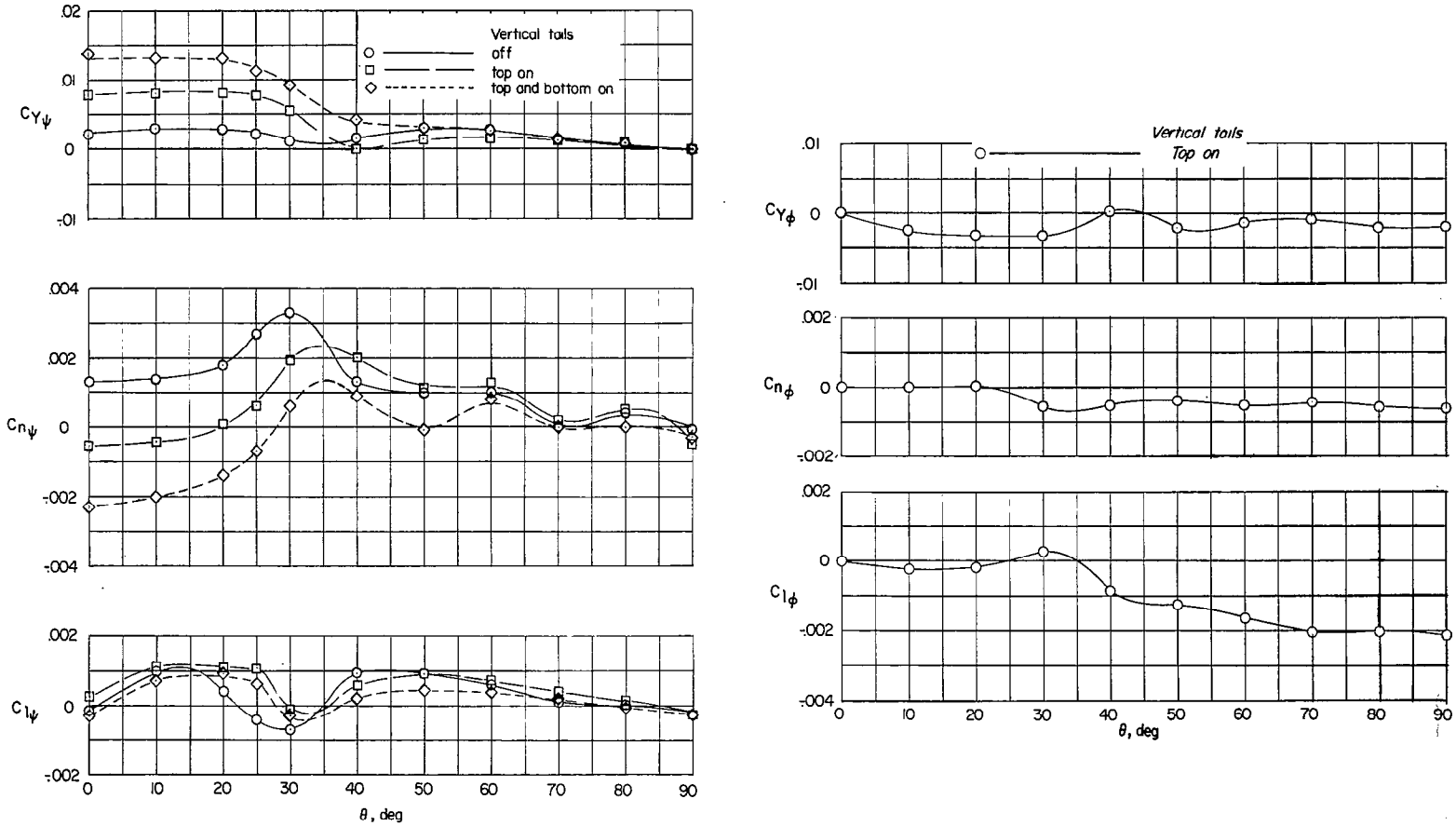

Figure 10.- Variation of yaw and roll derivatives, C_{Y_ψ}, C_{Y_ϕ}, C_{n_ψ}, C_{n_ϕ}, C_{l_ψ}, and C_{l_ϕ}, with angle of pitch.

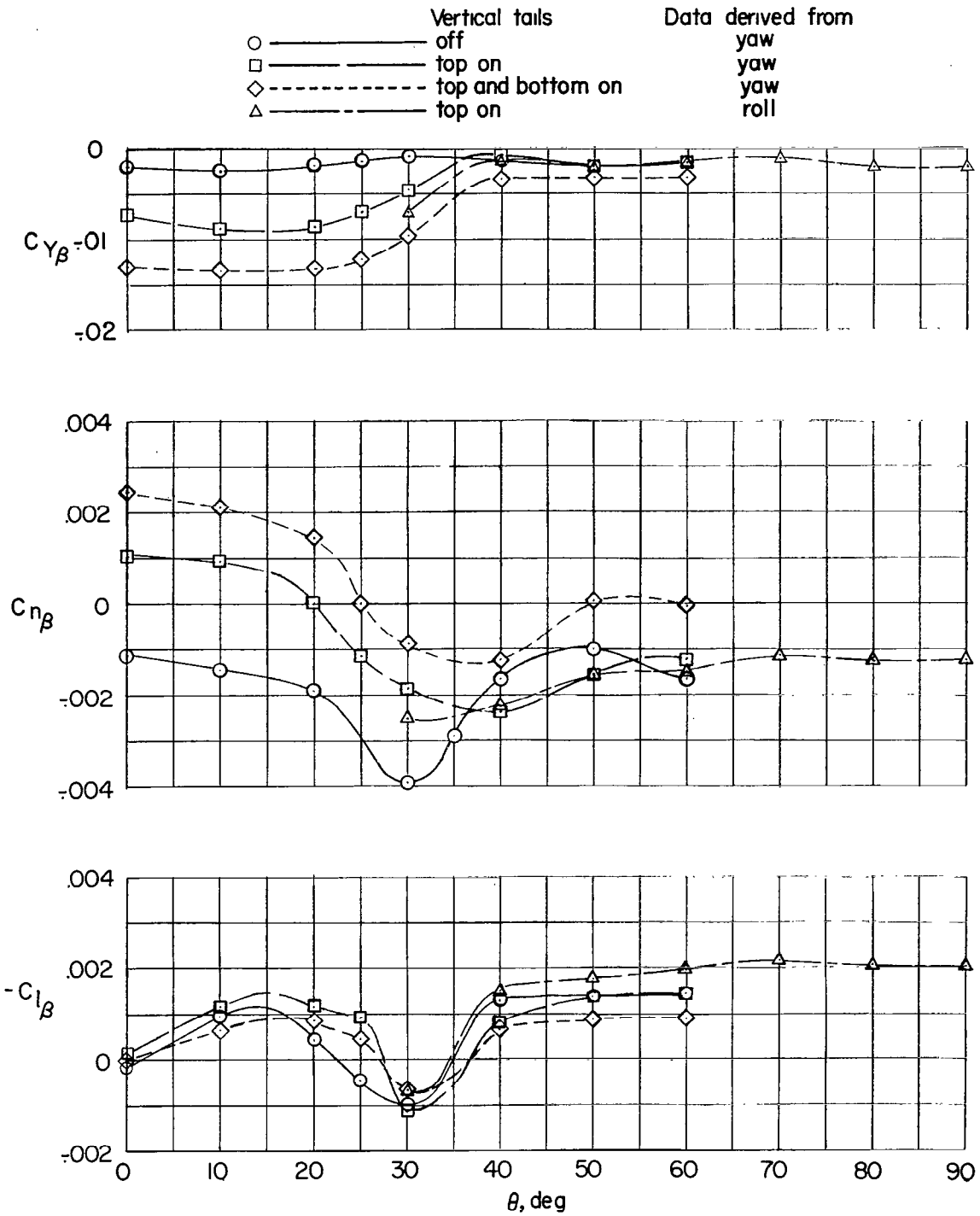

Figure 11.- Variation of the sideslip derivatives, C_{Y_β}, C_{n_β}, and C_{l_β}, with angle of pitch.

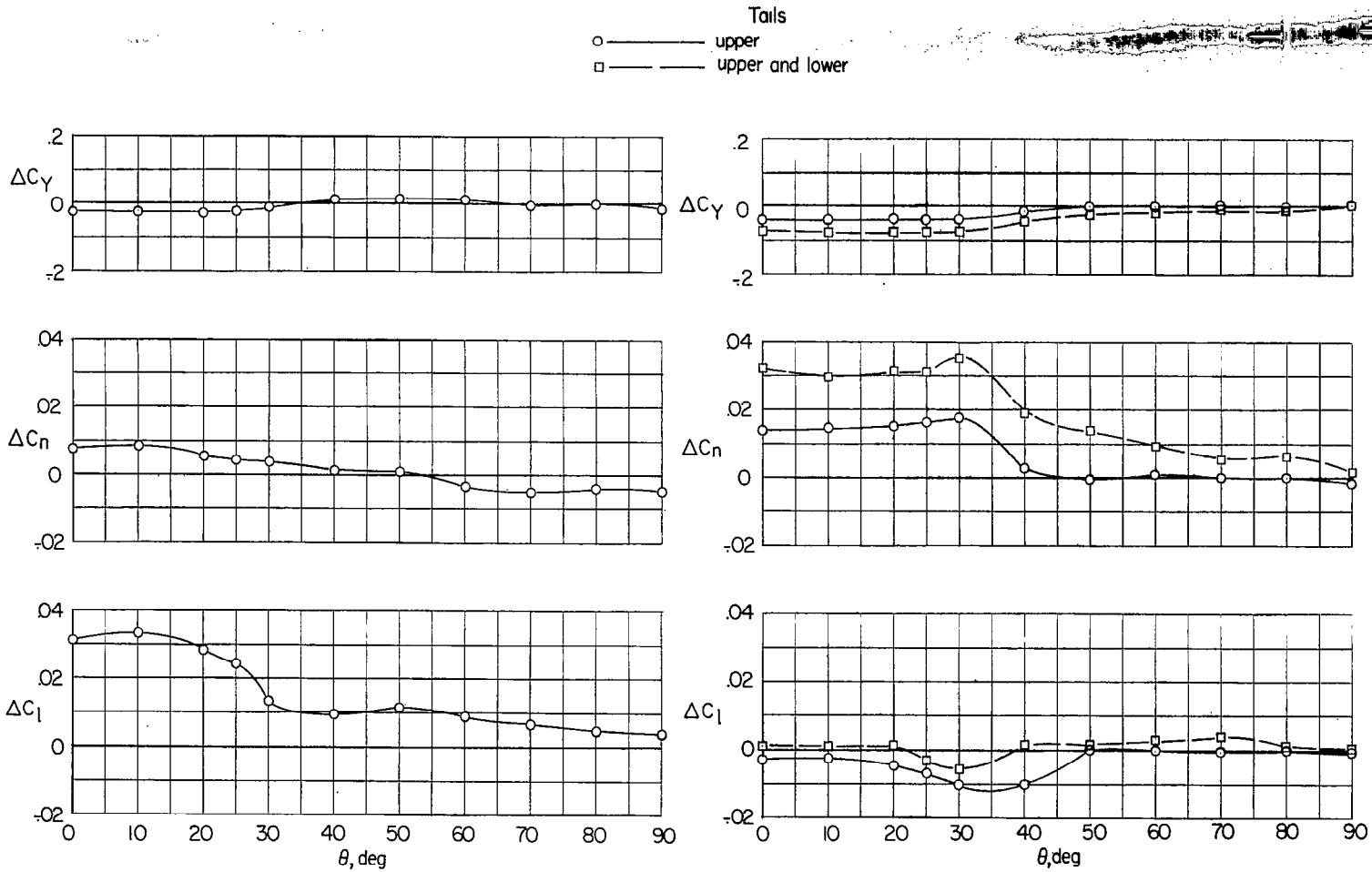

(a) Ailerons deflected 30° total ($\delta a_l = 15°$ and $\delta a_r = -15°$).

(b) Rudders deflected -25°.

Figure 12.- Increments in the lateral-force and moment coefficients produced by deflection of ailerons and rudders.

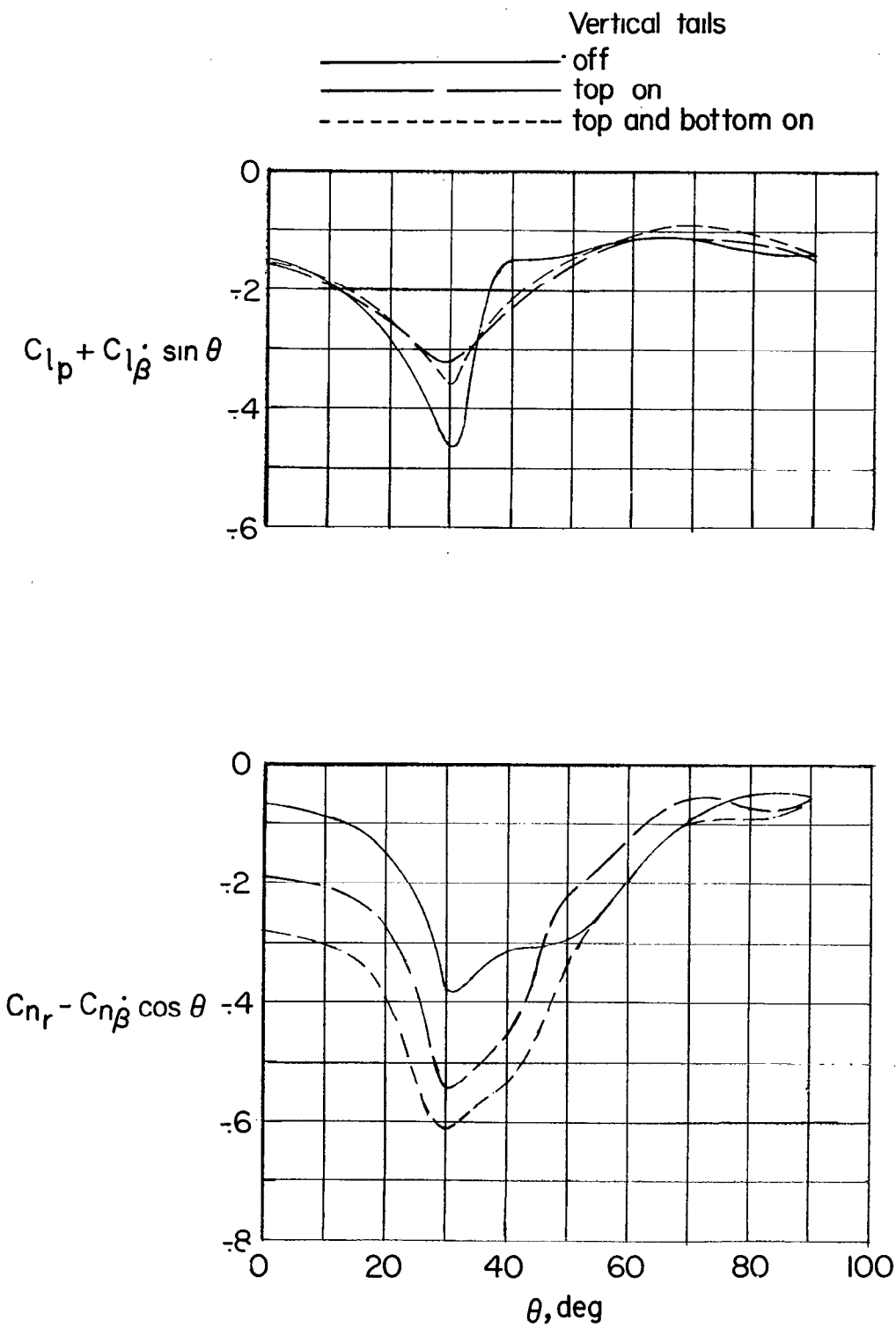

Figure 13.- Variation of the damping-in-roll and damping-in-yaw derivatives with angle of pitch.

NACA-Langley - 9-14-54 - 350